

<https://doi.org/10.15407/ujpe66.3.265>

L.A. BULAVIN, N.V. GAIDUK, M.O. REDKIN, A.V. YAKUNOV

Taras Shevchenko National University of Kyiv
(60, Volodymyrs'ka Str., Kyiv 01033, Ukraine; e-mail: yakunov@univ.kiev.ua)

SPECIFIC EFFECT OF MICROWAVES ON THE AQUEOUS SOLUTION OF RHODAMINE 6G ACCORDING TO FLUORESCENCE ANALYSIS

The effect of microwaves with a frequency of 2.45 GHz on the fluorescence of the aqueous solution of the organic dye rhodamine 6G has been studied. Deviations in the dynamics of the relative intensity and peak wavelength changes in the cases of microwave absorption and subsequent cooling of the solution, on the other hand, and contact heating and subsequent cooling, on the other hand, were registered. The obtained results are interpreted with the help of the percolation model. It is assumed that the electric component of the electromagnetic wave can directly affect the structure of the percolation cluster formed by the network of hydrogen bonds.

Keywords: microwave heating, fluorescence, organic dye, percolation model.

1. Introduction

Microwaves are electromagnetic radiation with the wavelength in vacuum ranging from 1 m (at a frequency of 300 MHz) to 1 mm (at 300 GHz). Rapid and controlled heating of a substance that absorbs microwaves, minimization of undesirable side effects, high energy efficiency, and ecological purity – all those factors favor the spread of microwave heating technologies in the chemical, food, electronic, and other industries [1].

However, it was repeatedly reported that the action of microwaves on some substances – in particular, aqueous systems – can lead to results that differ from those obtained at ordinary (contact or convective) heating [2–7]. In such cases, they talk about “specific” and/or “non-thermal” microwave effects. Their identification and explanation are the subject of lively discussions [8–13].

Specific effects are a result of some unique temperature phenomena that accompany the microwave heating. They include the effect of solvent overheating, selective heating, the emergence of “hot spots”, temperature gradients at the interface of two media, and so on. Besides obvious or predictable consequences of a specific action that can be explained at least qualitatively, sometimes the so-called “memory” phenom-

ena are observed. Namely, some properties acquired by the irradiated object during the microwave heating are kept unchanged for a certain time interval [2,6,7]. Typical relaxation processes in aqueous media have a characteristic time of an order of picoseconds, and the following question remains open: Which processes can be responsible for such a slow dynamics?

The term “non-thermal effects” is used to describe the effects of low-intensity microwaves, when the thermal effect can be neglected [4]. They are associated with the possibility of the direct action of an ac electric field on the matter. However, the molecular field strength (about 10^6 V/cm) is much higher than the field amplitude of typical microwave radiation sources, which makes the direct action of microwaves on molecules hardly probable. Moreover, microwave radiation is cannot substantially change the motion of ions because of their small absorption cross-section, as well as because of the viscosity of a liquid medium.

If the microwave power is rather high, the potentially possible non-thermal effects can be obscured against the background of specific effects and the ordinary heating. As a rule, those effects are detected by comparing the properties of a specimen before and after its exposure to microwaves. This approach requires a precise temperature control at the macro- and microlevels, as well as creating the identical conditions for heating and heat transfer. However, it re-

mains insufficiently informative to elucidate the primary mechanisms of microwave action.

Optical methods provide the possibility for simultaneous real-time monitoring of both the temperature and the state of the researched substance. In particular, fluorescence-based thermometry has satisfactory metrological parameters (sensitivity, performance, rate, spatial separation). Furthermore, this method is simple and safe [14], which makes it a convenient tool for the non-contact temperature control in the course of microwave heating. On the other hand, the fluorescence in a solution of dye molecules that can associate with one another by means of hydrogen bonds is very sensitive to the solvent structure, in particular, water [15, 16].

In the earlier works [17, 18], the absorption of millimeter-band electromagnetic waves in aqueous solutions was studied using the aqueous solutions of temperature-sensitive organic dyes. By performing the real-time registration of the changes in the relative fluorescence intensity, a local increase of the solution temperature in a capillary located in a rectangular waveguide was determined. As a result, certain quantitative differences were observed between the calculated temperature and the power of millimeter-band waves absorbed in the solution, which was measured using radio engineering facilities. Such differences may testify to the presence of additional factors, besides temperature-induced ones, affecting the influence of the electromagnetic field on the fluorescence of the aqueous solution.

In this work, the aqueous solution of the organic dye rhodamine 6G (R6G), which can form associates, was used for the temperature control of the solution during its rapid heating in a household microwave oven. The measurements were carried out by monitoring the relative intensity and the peak wavelength. To detect possible anomalies, the dynamics of spectrum parameters registered at ordinary (contact) and microwave heating was compared.

2. Temperature-Dependent Fluorescence Parameters

The fluorescence phenomenon is explained at the qualitative level making use of the classical Jablonski diagram [19]. A molecule in the ground state A^0 absorbs a light quantum $h\nu_{\text{abs}}$ and transits into the excited state A^* . Two scenarios of the further energy conversion are the most probable:

(1) the excited molecule returns back to the ground state by emitting the energy quantum $h\nu_{\text{emi}}$ (the radiative transition, i.e. fluorescence),

(2) the excited molecule returns back to the ground state emitting no energy quantum, but releasing the corresponding heat amount ΔQ (the non-radiative transition).

The both scenarios are characterized by the probabilities k_r and k_n , respectively. The parameters used to describe fluorescence often depend on the temperature [14, 20].

The absolute quantum yield is equal to the probability that the absorption of a photon by a fluorophore molecule will result in the fluorescence radiation emission:

$$\eta = \frac{k_r}{k_r + k_n}.$$

So, any factors that affect the probability of non-radiative processes, k_n , also affect the absolute quantum yield. In particular, the quantum yield depends on the chemical composition and the spatial structure of the molecule, the solvent, the presence of impurities, the temperature, and so on. In most cases, the temperature growth reduces the fluorescence quantum yield. As the temperature increases, the frequency and energy of molecular collisions in the solution become higher, as well as the amplitude of intramolecular vibrations, which leads to the growth of non-radiative relaxation of excited levels and, accordingly, to the fluorescence quenching.

At the same time, there are mechanisms that enhance the fluorescence yield as the temperature grows [21]. In particular, some organic molecules have a tendency to form bound complexes in solutions – dimers, trimers, *etc.* – for which the quantum yield is much lower than that for separate molecules (monomers) [22]. At sufficiently high solution concentrations, the fluorescence spectrum is formed as a linear superposition of the spectra emitted by molecular monomers and their associates. In turn, as the solution temperature increases, the associates decay into separate molecules, and this process is accompanied by a relative increase of the fluorescence yield. Typically, instead of the absolute quantum yield, the relative fluorescence intensity is measured, which is directly proportional to the relative quantum yield.

The wavelength corresponding to the maximum in the spectral contour, i.e. the peak wavelength λ_{max}

in the fluorescence spectrum, depends on the temperature. This dependence is called the thermochromic shift. The thermochromic effect is a result of the solvatochromic effect, i.e. the influence of the solvent polarity at the peak wavelength.

Fluorophores emit at frequencies that are lower than the frequencies, at which absorption occurs. The energy losses taking place between the absorption and radiation processes are characterized by the Stokes shift, i.e. the difference (in the energy or frequency units) between the positions of the maxima of the same electronic transition in the absorption and radiation spectra. The Stokes shift appears owing to certain dynamic processes, in particular, the dissipation of the vibrational energy, redistribution of electrons in solvent molecules, changes in the fluorophore dipole moment, reorientation of solvent molecules, and so forth.

In most organic fluorophores, the Stokes shift increases with the polarity, which leads to the radiation emission at lower energies (frequencies). This energy difference (reckoned in cm^{-1} units) depends on the refractive index n and the dielectric constant ε of the solvent and, in the first approximation, is described by the Lippert equation [19]

$$\bar{\nu}_{\text{abs}} - \bar{\nu}_{\text{emi}} \sim \left(\frac{\varepsilon - 1}{2\varepsilon + 1} - \frac{n^2 - 1}{2n^2 + 1} \right),$$

where $\bar{\nu}_{\text{abs}} = \lambda_{\text{abs}}^{-1}$ and $\bar{\nu}_{\text{emi}} = \lambda_{\text{emi}}^{-1}$, are the absorption and radiation, respectively, wave numbers (in cm^{-1} units). From this relation, it follows that an increase in the solvent polarity shifts the fluorescence spectrum toward the low-frequency (long-wavelength) region. Below for convenience, we will use the quantity $\bar{\nu}_{\text{max}}$ reciprocal to the peak wavelength, $\bar{\nu}_{\text{max}} = \lambda_{\text{max}}^{-1}$.

The thermochromic shift of the fluorescence spectrum occurs due to a change in the solvent polarity with the temperature. If the typical temperature dependences of the dielectric constant and the refractive index of solvents are taken into account, it turns out that the solvent polarity decreases, as the temperature increases. Therefore, the fluorescence spectrum shifts toward the high-frequency (short-wave) region with the temperature growth.

The quantum yield and the peak wavelength are mutually independent spectral parameters. They can be used to control the temperature either simultaneously or separately, depending on the experimental

capabilities, the temperature interval, and the type of an experimental specimen. The character of the temperature dependence of each parameter is associated with certain properties of the solvent. The independent control of those parameters and the comparison of their dynamic profiles can be a convenient tool for detecting subtle effects accompanying the heating of the medium, in particular, under microwave irradiation.

3. Materials and Methods

The specimens were prepared on the basis of the organic dye R6G and distilled water of high-performance liquid chromatography (HPLC) grade from the ALFARUS company (Kyiv, Ukraine). The solution concentration was about 0.4 g/l, which corresponded to the optimal ratio between the temperature sensitivity and the fluorescence intensity [21].

A semiconductor laser generating the radiation with a wavelength of 406 nm and an output power of 60 mW was used as an excitation source. The laser beam was focused using a lens into a cylindrical glass cell (the diameter $d = 10$ mm and the height $h = 50$ mm) filled with the solution. The fluorescence signal was directed to the input slit of a low-dispersion monochromator. In the output plane of the latter, there was arranged a light-sensitive matrix of a KAYTON USB-camera with a resolution of 640×360 pixels. The angle between the directions of the direct and secondary light rays was equal to 90° .

For the temperature calibration of the fluorescence spectrum parameters, the cuvette with the dye solution was placed in a massive copper heater that provided the rapid and almost uniform heating in a controlled mode. The solution temperature was monitored with the help of a miniature thermocouple mounted near the excitation region and connected to a digital multimeter. The temperature was measured every 0.5 s and the corresponding data were sent to the USB port of a PC. The spectra were registered at identical time intervals and processed in the batch mode using the ImageJ soft program, for which the necessary plugins were created.

The same optical scheme was used to register the dynamics of the microwave heating. The cuvette with the solution was placed in a 700-W microwave oven Elenberg MS-1400M near its front wall with a protective grid. At the first stage, the protective grid re-

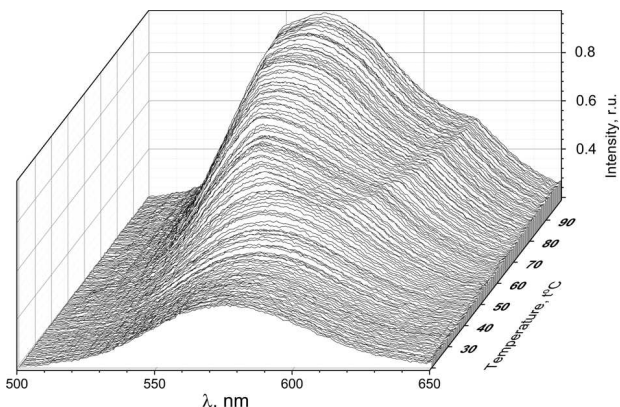


Fig. 1. Fluorescence spectra of the aqueous R6G solution registered, when the temperature increased from 20 to 100 °C

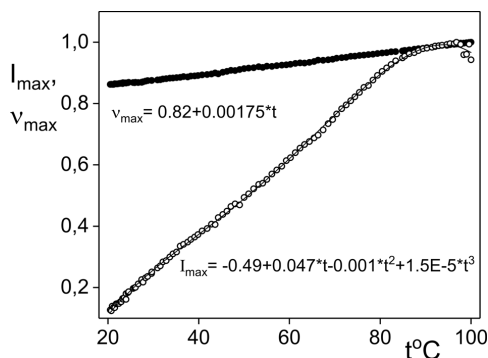


Fig. 2. Normalized temperature dependences of the relative intensity and the peak wavelength

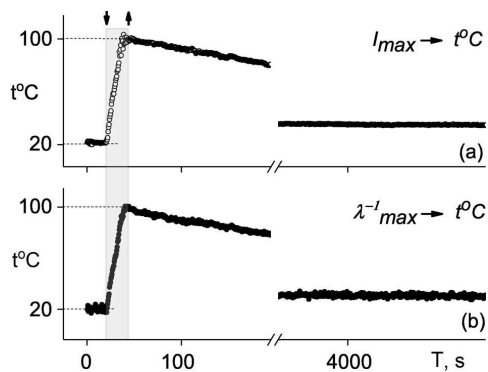


Fig. 3. Dynamic temperature profiles at the microwave heating and subsequent cooling determined on the basis of the relative intensity (a) and peak wavelength (b). The arrows mark the time moments of the microwave generator switching-on and -off

duced the fluorescence signal, but every time an additional adjustment of the optical scheme allowed the signal to be enhanced to an acceptable level.

4. Experimental Results

For the temperature calibration, the fluorescence spectra of aqueous R6G solutions were recorded at time intervals of 0.5 s as the temperature was uniformly increased from 20 to 100 °C. Figure 1 demonstrates a set of digitized spectra, where their temperature dependence can be well traced.

The temperature dependences of two spectrum parameters, I_{max} and λ_{max}^{-1} , normalized to their values at 100 °C are shown in Fig. 2. In the temperature interval $t = 20 \div 80$ °C, the relative fluorescence intensity has a high temperature sensitivity and therefore is the optimal parameter for the temperature control far from the boiling point. At $t > 80$ °C, the contribution of the temperature-induced quenching of the fluorescence of monomers becomes noticeable, and the temperature sensitivity is substantially reduced. Approximately to $t = 95$ °C, the relative fluorescence intensity is characterized by a low fluctuation level. At higher temperatures, this parameter increases considerably owing to the influence of optical inhomogeneities, the presence of which is typical of liquids near their boiling point. Within the whole temperature interval, the temperature dependence of the relative intensity can be satisfactorily approximated by the cubic polynomial

$$I_{max} = -0.49 + 0.47t - 0.001t^2 - 1.5 \times 10^{-5}t^3.$$

The inverse peak wavelength depends linearly on the temperature within the interval $t = 20 \div 100$ °C,

$$\lambda_{max}^{-1} = 0.8 + 0.00175t,$$

with relatively small deviations from this dependence.

Figure 3 illustrates a typical dynamics of the temperature variation in an aqueous R6G solution under the microwave heating and subsequent cooling. Two plots correspond to the dynamic profiles reproduced making use of the calibration curve (see Fig. 2) either for the relative intensity (panel a) or the peak wavelength (panel b). The dynamic profiles are almost identical except for a region near the boiling point.

A comparison of the temporal temperature profiles $t(T)$ (Fig. 3) with their counterparts obtained while making calibration for the ordinary heating showed that they are different, which is associated with different courses and rates of the relevant heat transfer processes. For the comparison between the dynamics of spectrum parameters obtained from two

dependences, $I_{\max}(T)$ and $\lambda_{\max}^{-1}(T)$, to be more correct, the time T (and, accordingly, the temperature t) was excluded and the dependence $I_{\max}(\lambda_{\max}^{-1})$ was obtained. Figure 4 demonstrates a typical pair of such dependences for the ordinary (contact) and microwave heating. For the contact heating (panel *a*), the dependence $I_{\max}(\lambda_{\max}^{-1})$ corresponds to the calibration curves (Fig. 3), whereas the microwave heating is accompanied by a faster change of λ_{\max}^{-1} in comparison with that of I_{\max} in the first phase of the process (20–50 °C), and its slowdown in the second one (50–100 °C).

Another specific feature of the microwave action on the fluorescence in the aqueous R6G solution can be revealed, if we compare the dependences $I_{\max}(\lambda_{\max}^{-1})$ obtained at the heating and subsequent cooling. In the case of contact heating (Fig. 5, *a*), the forward and reverse processes are expectedly accompanied by a synchronous change of both fluorescence spectrum parameters. At the same time, the microwave heating results in an appreciable discrepancy between the behavior of those parameters (Fig. 5, *b*). When cooling down from 100 to 50 °C, the quantity λ_{\max}^{-1} decreases faster than I_{\max} does. Afterward, the tendency for both parameters to return to their initial values is observed. This discrepancy can be interpreted as a specific memory effect of the solution with respect to the microwave irradiation.

5. Discussion

Anomalies in the dynamics of the fluorescence spectrum parameters for the aqueous solution R6G subjected to the microwave heating and subsequent cooling testify that, besides the temperature influence of microwaves on the solution, there is another one. In the case of heating, this effect is associated with the direct action of microwaves on the running processes in the irradiated specimen, whereas, at the cooling, it is determined by certain properties of the substance acquired under the microwave action. Let us consider those cases separately.

For the contact and microwave heatings (Fig. 4), the initial (at 20 °C) and final (at 100 °C) fluorescence spectrum parameters coincide, but the dynamics of their changes is somewhat different. In the case of contact heating, it corresponds to the calibration curve (taking the linear dependence $\lambda_{\max}^{-1}(t)$ into account). The action of microwaves leads to a

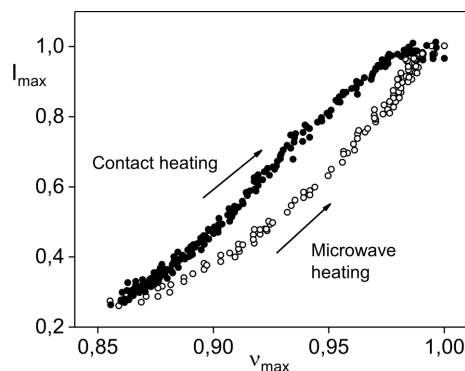


Fig. 4. Typical dependences “relative intensity versus peak wavelength” at the contact and microwave heatings

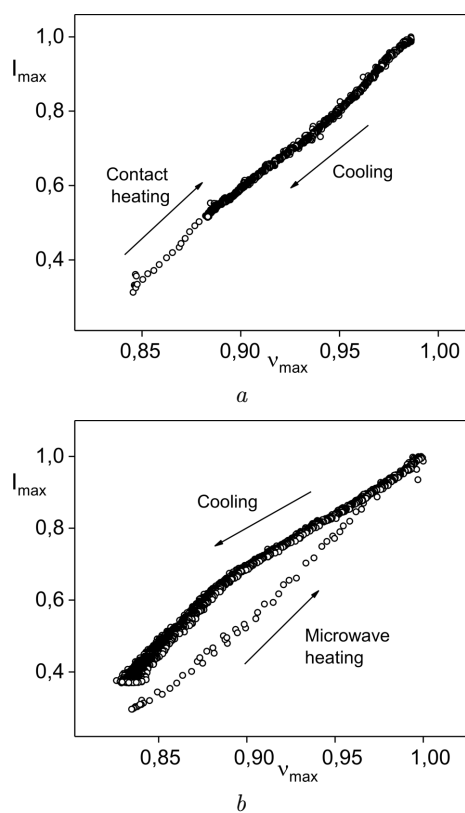


Fig. 5. Typical dependences “relative intensity versus peak wavelength” at the contact (*a*) heating-cooling and microwave (*b*) heating-cooling

more rapid growth of λ_{\max}^{-1} in comparison with I_{\max} at the first stage (approximately up to 50 °C), whereas this growth becomes slower at the second stage (50–100 °C).

In the framework of simple physical models, the non-thermal effect of microwaves on liquid systems is

explained by either of two direct mechanisms of the electric component action:

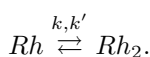
(a) changes in the solvent polarity as a result of the additional (superthermal) swinging of molecular dipoles,

(b) changes in the orientation of polar molecules that are directly involved in the internal chemical reactions [13].

According to our experimental results, the both scenarios remain possible under the microwave heating, and they are responsible for the difference between the dynamics of the fluorescence spectrum parameters in the microwave and contact heating cases.

For instance, at relatively low temperatures (up to 50 °C), the electric component of the microwave field reorients polar molecules and, in addition to the thermal factor, reduces the polarity of the aqueous matrix, which leads to a faster growth of λ_{\max}^{-1} . At high temperatures, a competition between two factors affecting the polarization – the temperature (chaotic) and electrically induced (partially ordered) ones – can be observed up to about 100 °C, where the former becomes dominant.

The relative fluorescence intensity of the R6G solution is determined by the concentration ratio between monomers and dimers, which are in the dynamic equilibrium at any temperature,



The kinetic parameters k and k' are determined by the Arrhenius law

$$k = A \exp\left(-\frac{E_a}{Rt}\right),$$

where the constant A depends on the collision frequency of molecules, E_a is the activation energy depending on the relative orientation of the molecules participating in the reaction, and R is the gas constant. The reaction rate and, as a result, the fluorescence intensity can be governed by both the temperature and the direct influence of the electric field [12]. At relatively low temperatures, the influence of the latter on the activation energy dominates over the thermal effect. With the increasing temperature, the situation becomes opposite.

Therefore, the comparison of the change dynamics obtained for the fluorescence spectrum parameters of

the aqueous R6G solution subjected to the ordinary and microwave heating gives us ground to assert that there is an additional factor, besides the temperature one, which is responsible for the microwave effect. However, it does not allow us to clarify its mechanism.

Let us consider the change dynamics of spectrum parameters at the cooling. The irreproducibility of the dependence $I_{\max}(\lambda_{\max}^{-1})$ at the microwave heating and subsequent cooling testifies that the aqueous R6G solution acquires new properties under the microwave irradiation, and those properties remain preserved for at least $\Delta T \sim 10^3$ s. At $t \leq 100$ °C, the non-temperature factor, which is responsible for those properties, becomes obscured against the background of the temperature-induced one because the fluorescence spectrum parameters coincide in this area for both heating methods.

At the cooling, the direct action of microwaves is absent, so the “chemical” mechanism [mechanism (b)] should be discarded. Moreover, the energy of single microwave photons (for example, a photon with a frequency of 3 GHz has an energy of 10^{-3} eV) is several orders of magnitude lower than the energy of chemical bonds, so that the processes like photochemical transformations can be ignored.

In works [2, 6, 7], a possibility for microwaves to affect the structure of the hydrogen bond network, which is preserved for a long time interval after the action of external factor has terminated, was considered. In the framework of the percolation model [23, 24], the structure of the aqueous matrix can be quantitatively described by introducing the density function for vibrational states, which is related to the fractal dimensionality D_F of the equivalent percolation cluster. In the equilibrium state, D_F explicitly depends on the temperature, in accordance with an analogous dependence for the average number of hydrogen bonds per H_2O molecule, n_H . Under the action of external factors, the value of n_H may change quite quickly, whereas D_F changes much more slowly because of bulk effects. In particular, model calculations for a two-dimensional percolation cluster spatially confined to a square $N \times N$ section gave the dependence $\tau \sim \sqrt{N}$ for the relaxation time [25].

In work [7], the mechanisms of microwave influence that could change the structure of the hydrogen bond network were reviewed. In particular, such changes may take place due to the appearance of a local electric charge induced by an external electric field in a

group of molecules, which results in a change additional to the temperature-induced one of the solvent polarity. The possibility of a synchronous cumulative influence of the coherent electric field of a standing microwave on the molecules in the medium is also assumed, which results in the reconstruction of hydrogen bonds irrespective of the fact that the external field amplitude is much smaller than the molecular field strength [26].

On the other hand, the efficiency of association processes of R6G molecules depends on the parameters of the supramolecular (cluster) structure of water [15, 27, 28]. By assuming that microwaves destroy or deform the percolation cluster, one may expect that the effective distance between fluorophore molecules – the parameters in the Arrhenius formula depend on it – should enlarge. As a result, the number of bound molecules, i.e. dimers, decreases and the fluorescence intensity, which is a kind of the supramolecular structure indicator, increases.

According to the character of the dependence $I_{\max}(\lambda_{\max}^{-1})$ at the first stage (100–50 °C) of the R6G solution cooling after the microwave heating, the structural relaxation is slower than the polarity relaxation, which can be interpreted as a manifestation of the percolation cluster memory with respect to the microwave action. The time interval $\Delta T \sim 10^3$ s within which such a delay is observed in the case of the aqueous R6G solution is substantially shorter than the values of analogous temporal parameters ($\Delta T > 10^5$ s) registered, when pure water was irradiated with microwaves [2, 6, 7]. Such a difference may probably be associated with the fact that the dye molecules stabilize the cluster structure of the solution by their own hydrogen bonds so that the solution becomes less sensitive to external factors.

6. Conclusions

The influence of microwaves with a frequency of 2.45 GHz on the fluorescence in the aqueous solution of the organic dye rhodamine 6G has been studied. Discrepancies between the change dynamics of the relative intensity and the maximum wavelength of fluorescence registered at the microwave absorption and at the ordinary contact heating were revealed. Analogous discrepancies were also detected when cooling the specimen previously heated in two ways. The results obtained are interpreted in the framework of the percolation model. It is predicted that the electric

component of the electromagnetic wave can directly affect the structure of the percolation cluster that is formed by the hydrogen bond network.

1. A. Bekal, A.M. Hebbale, M. Srinath. Review on material processing through microwave energy. *IOP Conf. Ser.: Mater. Sci. Eng.* **376**, 012079 (2018).
2. R. Walczak, J. Dziuban. "Microwave memory effect" of activated water and aqueous KOH solution. In: *Proceedings of the 15th International Conference on Microwaves, Radar and Wireless Communications, 17–19 May 2004, Warsaw* (IEEE, 2004).
3. A. Coptly, Y. Neve-Oz, I. Barak, M. Golosovsky, D. Davidov. Evidence for a specific microwave radiation effect on the green fluorescent protein. *Biophys. J.* **91**, 1413 (2006).
4. Huang Kama, Xiaqing Yang, Wei Hua, Guozhu Jia, Lijun Yang. Experimental evidence of a microwave non-thermal effect in electrolyte aqueous solutions. *New J. Chem.* **33**, 1486 (2009).
5. G. Morariu, M. Miron, A.-M. Mita, L.-V. Stan. Microwaves electromagnetic field influence on pH. Theoretical and experimental results. *Rev. Air Force Acad.* No. 1, 45 (2009).
6. H. Parmar, A. Masahiro, K. Yushin, A. Yusuke, Ph. Chi, P. Vishnu, E. Geoffrey. Influence of microwaves on the water surface tension. *Langmuir* **30**, 9875 (2014).
7. A. Yakunov, M. Bilyi, A. Naumenko. Long-term structural modification of water under microwave irradiation: Low-frequency Raman spectroscopic measurements. *Adv. Opt. Technol.* **2017**, 1 (2017).
8. J. Jacob, L. Chia, F. Boey. Thermal and non-thermal interaction of microwave radiation with materials. *J. Mater. Sci.* **30**, 5321 (1995).
9. D. Stuerga, P. Gaillard. Microwave athermal effects in chemistry: A myth's autopsy: Part I: Historical background and fundamentals of wave-matter interaction. *J. Microw. Power Electromagn. Ener.* **31**, 87 (1996).
10. N. Kuhnert. Microwave-assisted reactions in organic synthesis: Are there any nonthermal microwave effects? *Angew. Chem. Int. Ed.* **41**, 1863 (2002).
11. C. Kappe, B. Pieber, D. Dallinger. Microwave effects in organic synthesis: Myth or reality? *Angew. Chem. Int. Ed.* **52**, 1088 (2013).
12. Boon Wong. Understanding nonthermal microwave effects in materials processing – A classical non-quantum approach. In: *Processing and Properties of Advanced Ceramics and Composites VI: Ceramic Transactions, Vol. 249* (The American Ceramic Society, 2014), p. 329.
13. P. Bana, I. Greiner. Interpretation of the effects of microwaves. In *Milestones in Microwave Chemistry* (Springer, 2016), Ch. 4.
14. J. Lou, T.M. Finegan, P. Mohsen, T.A. Hatton, P.E. Laibinis. Fluorescence-based thermometry: Principles and applications. *Rev. Analyt. Chem.* **18**, 235 (1999).
15. L. Levshin, A. Saletskii, V. Yuzhakov. Forms of aggregation of molecules of rhodamine dyes in mixtures of polar

- and nonpolar solvents. *Zh. Strukt. Khim.* **26**, 95 (1985) (in Russian).
16. A. Vasylieva, I. Doroshenko, Ye. Vaskivskiy, Ye. Chernolevska, V. Pogorelov. FTIR study of condensed water structure. *J. Mol. Struct.* **1167**, 232 (2018).
 17. N. Kuzkova, O. Popenko, A. Yakunov. Application of temperature-dependent fluorescent dyes to the measurement of millimeter wave absorption in water applied to biomedical experiments. *J. Biomed. Imag.* **2014**, 1 (2014).
 18. D. Babich, A. Kulsy, V. Pobiedina, A. Yakunov. Application of fluorescent dyes for some problems of bioelectromagnetics. In: *Proc. SPIE 9887, Biophotonics: Photonic Solutions for Better Health Care V* **9887**, 988735 (2016).
 19. J.R. Lakowicz. *Principles of Fluorescence Spectroscopy* (Springer, 2006).
 20. V. Degoda, A. Gumenyuk, I. Zakharchenko, O. Svechnikova. The features of the hyperbolic law of phosphorescence. *J. Phys. Stud.* **15**, 1 (2011).
 21. S. Viznyuk, P. Pashinin. The effect of temperature combustion luminescence in water solution of rhodamine 6G. *JETP Lett.* **47**, 190 (1988).
 22. K. Kristinaityte, A. Marsalka, L. Dagys, K. Aidas, I. Doroshenko, Y. Vaskivskiy, Y. Chernolevska, V. Pogorelov, N.R. Valeviciene, V. Balevicius. NMR, Raman, and DFT study of lyotropic chromonic liquid crystals of biomedical interest: Tautomeric equilibrium and slow self-assembling in sunset yellow aqueous solutions. *J. Phys. Chem. B* **122**, 3047 (2018).
 23. L. Bulavin, M. Bilyi, A. Maksymov, A. Yakunov. Peculiarities of the low-frequency Raman scattering by supramolecular inhomogeneties of hydrogen-bonded liquids. *Ukr. J. Phys.* **55**, 966 (2010).
 24. N. Kuzkova, A. Yakunov, M. Bilyi. Low-frequency Raman spectroscopic monitoring of supramolecular structure in H-bonded liquids. *Adv. Opt. Technol.* **2014**, 1 (2014).
 25. A. Yakunov, P. Yakunov. Slow dynamics of water structure in cellular automata model. In: *Proceedings of the International Conference "Physics of Liquid Matter: Modern Problems"* (2004), p. 140.
 26. H. Hinrikus, M. Bachmann, J. Lass. Understanding physical mechanism of low-level microwave radiation effect. *Int. J. Radiat. Biol.* **94**, 877 (2018).
 27. N. Domnina, A. Korolev, A. Potapov, A. Saletskii. Influence of microwave radiation on the association processes of rhodamine 6G molecules in aqueous solutions. *J. Appl. Spectrosc.* **72**, 33 (2005).
 28. V. Pogorelov, I. Doroshenko, G. Pitsevich, V. Balevicius, V. Sablinskas, B. Krivenko, L.G.M. Pettersson. From clusters to condensed phase—FT IR studies of water. *J. Mol. Liq.* **235**, 7 (2017).

Received 28.08.20.

Translated from Ukrainian by O.I. Voitenko

Л.А. Булавін, Н.В. Гайдук,
М.О. Редькін, А.В. Якунов

СПЕЦИФІЧНА ДІЯ МІКРОХВИЛЬ
НА ВОДНИЙ РОЗЧИН РОДАМІНУ 6G
ЗА ДАНИМИ ФЛЮОРЕСЦЕНТНОГО АНАЛІЗУ

Вивчено вплив мікрохвиль з частотою 2,45 ГГц на флуоресценцію водного розчину органічного барвника родаміну 6G. Зафіксовано відхилення в динаміці зміни відносної інтенсивності та пікової довжини хвилі під час поглинання мікрохвиль, а також під час подальшого охолодження розчину порівняно із контактним нагріванням. Результати інтерпретовано в рамках перколяційної моделі. Передбачається, що електрична складова електромагнітної хвилі може безпосередньо впливати на структуру перколяційного кластера, який формується сіткою водневих зв'язків.

Ключові слова: мікрохвильове нагрівання, флуоресценція, органічний барвник, перколяційна модель.